Proc. 15th Int. Symp. Origin of Matter and Evolution of Galaxies (OMEG15)
JPS Conf. Proc. **31**, 011027 (2020)
https://doi.org/10.7566/JPSCP.31.011027

Neutrino self-interaction and MSW effects by an equi-partitioned Fermi-Dirac neutrino luminosity on the supernova neutrino-process

Heamin Ko[1], Myung-Ki Cheoun[1], Motohiko Kusakabe [2], Takehito Hayakawa [3], Hirokazu Sasaki [4], Toshitaka Kajino [2,4], Grant J. Mathews [5]

[1]*Department of Physics and OMEG institute, Soongsil University, Seoul 156-743, Republic of Korea*
[2] *School of Physics and International Research Center for Big-Bang Cosmology and Element Genesis, Beihang University, Beijing 100083, China*
[3]*National Institutes for Quantum and Radiological Science and Technology, 2-4 Shirakata, Tokai, Naka, Ibaraki 319-1106, Japan*
[4]*The University of Tokyo, Bunkyo-ku, Tokyo 113-0033, Japan and National Astronomical Observatory of Japan, Mitaka, Tokyo 181-8588, Japan*
[5]*Department of Physics, Center for Astrophysics, University of Notre Dame, Notre Dame, IN 46556, USA*

E-mail: cheoun@ssu.ac.kr

(Received November 6, 2019)

We investigate nuclear abundances produced from the neutrino (ν)-process in supernova explosions. By adopting an equi-partitioned ν-luminosity for each neutrino flavor, we have calculated the ν-flux propagation including both its modification by ν self-interaction (ν-SI) near the ν-sphere and the Mikheyev-Smirnov-Wolfenstein (MSW) effect in the outer O-Ne-Mg layer. The abundances of heavier isotopes ^{92}Nb, ^{98}Tc and ^{138}La are largely enhanced by the ν-SI for the inverted mass hierarchy. The ratio of ^{7}Li/^{11}B is lower in the inverted hierarchy than in the normal hierarchy.

KEYWORDS: neutrino process, neutrino self-interactions, neutrino oscillation

The neutrino (ν)-process is the nucleosynthesis mechanism induced by the neutrinos produced in core-collapse supernova (SN) explosions [1, 2]. It only affects the abundances of some rare nuclei, such as ^{7}Li and ^{11}B [3, 4], ^{19}F [5], ^{92}Nb [6] and ^{98}Tc [7], and ^{138}La, and ^{180}Ta [2, 8], termed as ν-isotopes. A comparison of calculated ν-process abundances with observational abundances or meteoritic analyses can provide valuable information on the associated ν physics and supernova physics [2, 9–11]. For example, recent progress of meteoritic analyses has revealed the ratios at the solar system formation, ^{92}Nb/^{93}Nb $\simeq 10^{-5}$ [12] and ^{98}Tc/^{98}Ru $< 6 \times 10^{-5}$ [13]. The previous studies also show that the ν-isotopic abundances are sensitive to neutrino energy spectra and that the ν process is a probe of the neutrino physics in the SN explosion.

However, there still remain some ambiguities in treating the ν interactions. One example is the ν mass hierarchy (MH), i.e., the normal hierarchy (NH) versus the inverted hierarchy (IH). The neutrino MH strongly affects the ν-flux and the subsequently produced ν-process abundances [4]. Another example is the matter enhanced ν oscillations, i.e., the MSW effect which gives rise to additional ν mixing from that of free space around the bottom of the C/O-rich layer [3,4]. A third important aspect is the ν self-interaction (ν-SI) arising from ν-ν scattering [14, 15]. This is usually negligible, but near to the ν-sphere the ν-density approaches 10^{32}cm^{-3} according to a Fermi-Dirac (FD) distribution [16]. This density is large enough that the ν-SI should be taken into account for the estimation of the ν-flux. In this paper, we report on the first ever systematic investigation of the ν-SI as well as the MSW effects on the ν-process.

All of the modifications due to the ν-SI and the matter effect in the propagating neutrino flux can be taken into account by solving the following evolution equation for the ν density matrix [14, 15]

$$\begin{aligned}\dot{\rho}_{\mathbf{p}} &= +\frac{1}{2E}[M^2,\rho_{\mathbf{p}}] + \sqrt{2}G_F[L,\rho_{\mathbf{p}}] + \sqrt{2}G_F\Sigma_{\mathbf{q}}(1-\cos\theta_{\mathbf{pq}})[(\rho_{\mathbf{q}}-\bar{\rho}_{\mathbf{q}}),\rho_{\mathbf{p}}]\,, \\ \dot{\bar{\rho}}_{\mathbf{p}} &= -\frac{1}{2E}[M^2,\bar{\rho}_{\mathbf{p}}] + \sqrt{2}G_F[L,\bar{\rho}_{\mathbf{p}}] + \sqrt{2}G_F\Sigma_{\mathbf{q}}(1-\cos\theta_{\mathbf{pq}})[(\rho_{\mathbf{q}}-\bar{\rho}_{\mathbf{q}}),\bar{\rho}_{\mathbf{p}}]\,.\end{aligned} \tag{1}$$

Here, $M^2 = U\Delta m^2 U^+$ with the PMNS mixing unitary matrix U is the neutrino mass-matrix including the vacuum oscillations, $\mathbf{p}$ and $\mathbf{q}$ are the momenta of the propagating and background neutrinos. The neutrino density matrix ρ and the charged lepton number density matrix L are given by

$$\rho = \begin{pmatrix} \langle\nu_e|\nu_e\rangle & \langle\nu_e|\nu_\mu\rangle & \langle\nu_e|\nu_\tau\rangle \\ \langle\nu_\mu|\nu_e\rangle & \langle\nu_\mu|\nu_\mu\rangle & \langle\nu_\mu|\nu_\tau\rangle \\ \langle\nu_\tau|\nu_e\rangle & \langle\nu_\tau|\nu_\mu\rangle & \langle\nu_\tau|\nu_\tau\rangle \end{pmatrix},\quad L = \begin{pmatrix} N_e - N_{\bar{e}} & 0 & 0 \\ 0 & N_\mu - N_{\bar{\mu}} & \\ 0 & 0 & N_\tau - N_{\bar{\tau}} \end{pmatrix}, \tag{2}$$

where $\langle\nu_\alpha|\nu_\beta\rangle = \sum_\gamma \langle\nu_\alpha|\nu_\gamma(t)\rangle\langle\nu_\gamma(t)|\nu_\beta\rangle$ with neutrino flavors α and β. $N_{x(=e,\mu,\tau)}$ denotes lepton number density. The 1st and 2nd terms on the r.h.s. of Eq. (1) describe ν oscillations in vacuum and an additional matter effect, respectively. The electron number density is calculated with a constant electron fraction w.r.t. the baryon density given by a hydrodynamics model [17]. The muon and tau densities are assumed to be negligible in this work. The non-linear ν-ν scattering term is taken into account in the 3rd term.

The evolution of the ν-flux by the ν-SI is achieved by solving Eq. (1) for the ν distribution function, $f(r;\epsilon_\nu,T_{\nu_\alpha}) = f_{FD}(\epsilon_\nu,T_{\nu_\alpha})\langle\rho(r;\epsilon_\nu)\rangle$, which is normalized with the angle averaged ν-density matrix $\langle\rho(r;\epsilon_\nu)\rangle$. The differential ν-flux considered in this work is defined as follows

$$\frac{d}{d\epsilon_\nu}\phi_{\nu_\alpha}(t,r;\epsilon_\nu,T_{\nu_\alpha}) = \frac{L_\nu(t)}{4\pi r^2}\frac{\epsilon_\nu^2}{\langle\epsilon_\nu\rangle}f(r;\epsilon_\nu,T_{\nu_\alpha})\,, \tag{3}$$

where $L_\nu(t)$ is the ν luminosity. Initial conditions are adopted from the equi-partitioned luminosity for each ν-flavor based on a Fermi-Dirac distribution from Refs. [4, 18]. The ν luminosity is normalized at $t = 1\ s$ and the ν temperatures are taken as T_{ν_e}= 3.2 MeV, $T_{\bar{\nu}_e}$= 5 MeV and T_{ν_x}= 6 MeV ($\nu_x = \nu_\mu, \nu_\tau, \bar{\nu}_\mu$ and $\bar{\nu}_\tau$), respectively. Numerical results in Fig. 1 are obtained using a multi-angle approach as in Ref. [19]. They show how the ν-flux emitted from the ν-sphere is modified by the ν-SI.

The neutrino and electron densities near the ν-sphere play vital roles on the ν-process in the SN environment. For instance, if the electron density is much higher than the ν-density this causes a suppression of the ν-SI effect [20]. However, as the shock wave propagates, the electron density decreases, so that the flavor change by the ν-SI becomes significant in the outer region [21]. This implies that the ν-SI depends on the hydrodynamics and it becomes important to know the critical condition when the ν-SI becomes significant. Once the ν-flux is changed by the ν-SI, the flux distributions retain their shapes until they undergo the MSW effect.

The baryon matter density is described by the hydrodynamic evolution. It heavily depends upon the SN model employed. Although there are many SN hydrodynamics models, we adopt the phenomenological model of Fogli [17]. We take a density profile for the inner region approximated as a power law and assume that it remains valid for $t \le 1s$. Usually, the phenomenological model is obtained by a fitting to a realistic result from a hydrodynamics model. The SN model may have many uncertainties because of the artificial means employed to induce the explosion. In this context, the Fogli model is useful for initial conditions to study the roles of the ν physics in the SN nucleosynthesis.

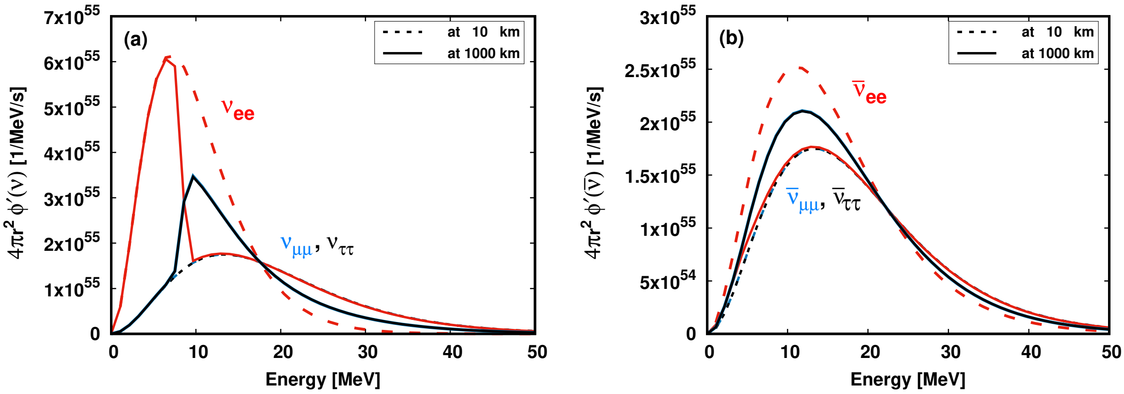

Fig. 1. Differential ν-flux for ν (a) and $\bar{\nu}$ (b) $\phi'(= d\phi/d\epsilon)$ modified by the ν-SI in the IH scheme. Dashed and solid lines show the initial flux at 10 km assumed to be FD and the final flux at 1000 km after the ν-SI, respectively.

Neutrinos in the inner region calculated by the Fogli density profile propagate from $r = 10$ km to 1000 km. Beyond that, the flux is unchanged by the ν-SI. We only calculate the IH case because the NH scheme exhibits very little ν-SI effect [19]. The ν_e ($\nu_{x=\mu,\tau}$) flux at 1000 km is lower (higher) than the original flux from the surface of ν-sphere in the energy range of $\sim 8-17$ MeV. However, the situation is reversed in the higher energy region above the point of equal flux for the three flavors. For the $\bar{\nu}_e$ and $\bar{\nu}_x$ flux case, one finds similar tendencies [19]. The energy- and time-dependence of the ν-flux affect the ν reactions because the reaction rates depend upon the ν-flux and incident energy [22].

Beyond the outer region above 2000 km where the ν-process is investigated in detail, the MSW effect plays a significant role. Therefore, we need the temperature and density profiles from the shock propagation. We utilize the pre-supernova (pre-SN) model of Refs. [23–25]. This model was developed for SN1987A. It is for a 16.2 $M_\odot$ progenitor with a 6 $M_\odot$ He core mass. It assumes a metallicity of $Z = Z_\odot/4$ which is much smaller than the solar metallicity of $Z_\odot = 0.019$ adopted in Ref. [2].

For the ν-process, we need ν-nucleus reaction cross sections. In this work we utilize the numerical results of Ref. [4] for the light nuclei. These were calculated in a few-body model for the ^{4}He reaction and in a shell-model for ^{12}C. For the heavy nuclei, ν-induced reactions are calculated in the quasi-particle random phase approximation through many multipole transitions dominated by the Gamow-Teller transition [26, 27].

Neutrino reaction rates in SN explosion are calculated as follows

$$\lambda_{\nu_\alpha}(r) = \frac{L_\nu(t)}{L_\nu(t_1)} \int_0^\infty \sum_{\beta=e,\mu,\tau} \frac{d\phi_{\nu_\beta}}{d\epsilon_\nu}(t_1, r = 1000\text{ km}; \epsilon_{\nu_\beta}) P_{\nu_\beta\nu_\alpha}(r; \epsilon_\nu)\, Br(\epsilon_\nu)\, \sigma_{\nu_\alpha}(\epsilon_\nu)\, d\epsilon_\nu\ . \tag{4}$$

Here $t_1 = 1$ s and $\phi_{\nu_\beta}(t, r; \epsilon_{\nu_\beta})$ is the ν_β-flux modified by the ν-SI. The ν reaction cross section, σ_{ν_α}, is multiplied by the branching ratio, $Br(\epsilon_\nu)$, of the excited states calculated using the statistical method [28]. The flavor transition probability, $P_{\nu_\beta\nu_\alpha}$, included the ν oscillations in matter based upon the mixing parameters in Ref. [29].

Other relevant nuclear reactions include the (n,γ) reactions on nuclei in the $A \sim 100$ mass region. We utilized the (n,γ) reaction data [30] for the explosive nucleosynthesis in which local systematics of the Hauser-Feshbach model parameters were carefully investigated to infer the theoretical prediction for the unstable nuclei to obtain the realistic abundances after the weak s-process [7].

In Fig. 2 (a), we show numerical results for the mass-fractions of ^{92}Nb, ^{98}Tc, ^{138}La and ^{180}Ta. Abundances obtained using a FD distribution without ν-SI are presented by dashed lines. Abundances of ^{92}Nb, ^{98}Tc, and ^{138}La decrease with increasing M_r except for valleys. This trend can be understood

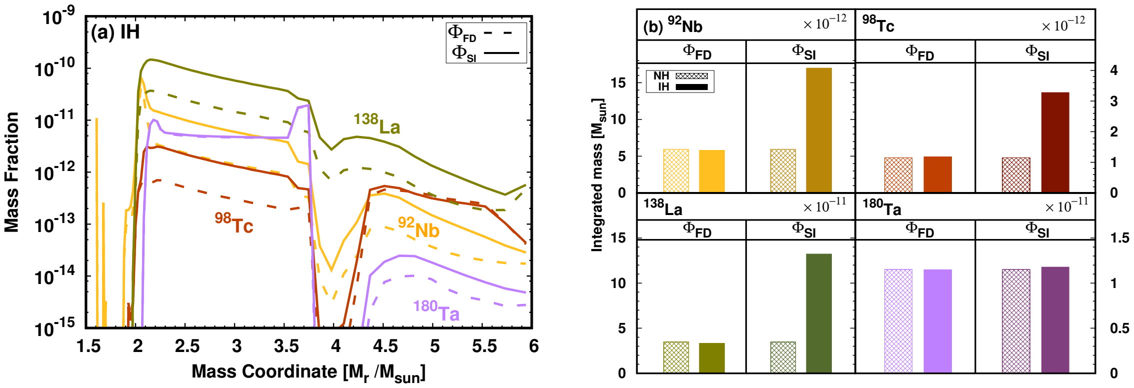

Fig. 2. Abundances (a) of ^{92}Nb, ^{98}Tc, ^{138}La and ^{180}Ta in the IH scheme and (b) their integrated masses. Solid and dashed lines are the results with and without the ν-SI, respectively.

by the general form of neutrino-induced reaction rate which is proportional to the neutrino flux scaling as r^{-2}. A valley around the $M_r \sim 4\ M_\odot$ region stems from strong destruction via the (n,γ) reactions behind the shock heating. Another valley in the region of $M_r < 2.0\ M_\odot$ comes from the photodisintegration of the pre-SN elements. These are almost identical to previously published results [6]. Abundances of ^{92}Nb, ^{138}La and ^{180}Ta are shown to be produced mainly inside the O-Ne-Mg layer ($\sim 2-4\ M_\odot$) by the ν-process as has been previously noted [2, 6]. In the outer region of $M_r \gtrsim 4.4 M_\odot$ the abundances come mainly from the ν-process.

Abundances for the ν-SI included case are denoted by solid lines. Most of the heavy nuclei are shown to be mainly produced inside the MSW region independently of the ν-flux type. Thus, the effect of ν-SI is observed in the abundances of heavy isotopes. The ν-SI increases the heavy element abundances throughout the whole stellar region, except for ^{180}Ta whose abundance was not changed by the ν-SI in the main production region. The increased abundances by the ν-SI are attributed to an increase of the ν-flux in the high energy region.

Figure 2 (b) shows integrated masses in the case with the ν-SI included compared to those without the ν-SI. Although most of the heavy nuclei are produced inside the MSW region, these ratios are also given for both MH schemes including the MSW effect. For the NH case, neither the ν-SI nor the MSW affects the heavy element abundances. This is because there is no discernible change of the ν-flux inside the ν-process region. In contrast, one can note interesting consequences of the MSW mixing and the ν-SI in the IH case. The ν-SI effect increases the ^{92}Nb, ^{98}Tc and ^{138}La abundances by a factor of three to four because of the high energy tail from the swapped ν spectra.

The insensitivity of the ^{180}Ta production to the ν-SI and the MH scheme and the constant abundance in the inner layer of $M_r = 2.2 - 3.5 M_\odot$ in Fig. 2 (a) come from the fact that, in the present pre-SN model, most of the ^{180}Ta are not produced via the ν-process. Rather it existed from the pre-SN stage.

Figure 3 shows the abundances of the light element, ^{7}Li and ^{11}B, including the ν-SI and the MSW effect. This figure illustrates that the main production regions are the outer region above the MSW layer from 4.5–5.5 $M_\odot$. Both elements are notably increased by the ν-SI. This is because the increased ν_e-flux in the high energy tails increases the ν reaction rates in the whole mass region $2.0 < M_r < 5.5$ $M_\odot$. If one ignores the ν-SI, the light nuclear abundances depend upon the MSW effect and the MH as discussed in Ref. [4]. This is because of the rapid change of the ν transition probability in the MSW region. Therefore, several previous papers [4, 9, 10] have argued for the possibility to deduce the ν MH from the light element abundances. In order to study the MSW effect [4] in detail, we present the results in the cases with and without the MSW effects. Both the FD and ν-SI results in Fig. 3 (a)

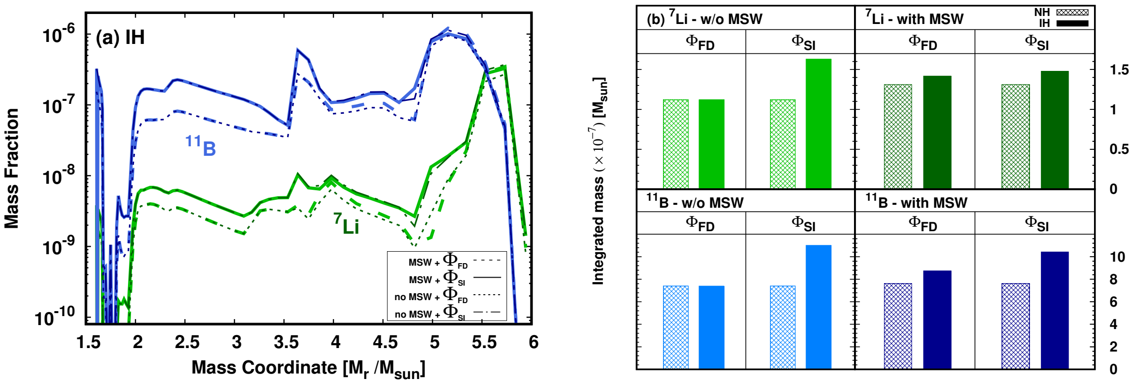

Fig. 3. Same as Fig. 2, but for ^{7}Li and ^{11}B. Abundances are plotted at 1 yr after the SN explosion. Solid and dashed lines show the results due to the ν-SI and the FD case with the MSW effect, respectively. Dotted and dotted-dashed lines are the abundances w/o the MSW effect.

show only a few percent deviation by the MSW effect over the whole mass region.

For a quantitative understanding, in Fig. 3 (b) we show explicitly the ν-SI and MSW effects on the total integrated masses. We note that the ν-SI effect does not change the integrated mass for the NH case (see hatched histograms). However, for the IH scheme, it increases the abundances by about 5 ~ 30% for ^{7}Li and ^{11}B. This comes from the high energy tails above 17 MeV in the ν_e-flux increased by the ν-SI. The ν-SI increases ^{7}Li and ^{11}B by about 5 and 20%, respectively when the MSW effect is included. Nevertheless, the ν-SI effect in light elements is much smaller than it is for the heavy elements.

One interesting point is that the IH scheme with the MSW effect always increases the abundances of both nuclei for a FD distribution. But, if the MSW and the ν-SI are switched on together, they are decreased by about 5% due to the MSW effect. This is because the flavor change at the MSW resonance converts the larger ν_e flux at high energies to a lower flux.

In a nutshell, the ν-SI does not affect the abundances for the NH case, but increases them for the IH case. The MSW effect increases (decreases) the abundances if we include the ν-SI in the NH (IH) scheme.

This trend could be understood by the contribution of ν_e. The contribution of CC reactions of ν_e dominates in production of ^{92}Nb, ^{138}La and ^{180}Ta. In contrast, in light ν-isotope synthesis, the CC reactions of $\bar{\nu}_e$ and NC reactions also have contributions of the same order of magnitude as that of CC ν_e reactions. Thus, the relatively small enhancements in ^{7}Li and ^{11}B abundances are understood simultaneously with those of heavy ν-isotopes consistently.

Finally, in Fig. 4, we illustrate the MH dependence of the light-element abundance ratio, ^{7}Li/^{11}B. Without the ν-SI, the MSW always increases this ratio [31]. However, with the ν-SI, the MSW either increases the ratio for the NH case, or decreases the ratio for the IH case. For the case with the MSW effect, the yield ratio is not changed by the ν-SI effect in the NH scheme while it is decreased by 20% in the IH scheme. It turns out that the NH choice predicts about 20 ~ 30% increase compared to the IH scheme. For reference, a constraint on the Li/B ratio of the SN yield estimated by the Bayesian analysis of the ratio data [10] is shown in this figure. This constraint is derived under the assumption that the observed presolar grains formed from well-mixed matter with solar composition and fully-mixed supernova ejecta. For further analysis of the MH, we need more accurate meteoritic data with certain detections of anomalies in ^{7}Li and ^{11}B isotopic ratios.

In conclusion, we have included for the first time the effects of both the ν-SI and MSW mixing on ν-process nucleosynthesis in SN explosions. The ν-flux was evaluated by solving the evolution

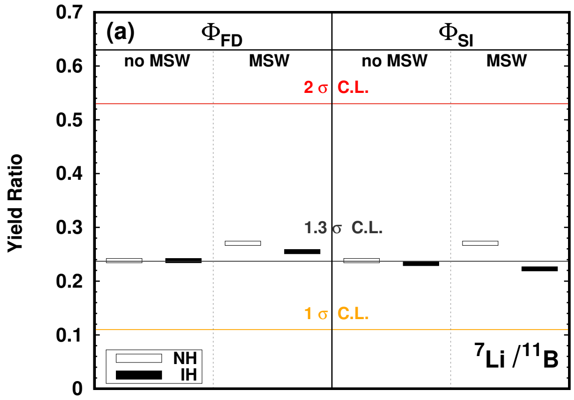

Fig. 4. Ratios of the abundance of ^{7}Li to ^{11}B for various cases of the MSW, ν-SI and the MH scheme. The width of each band represents a presumed few percent uncertainty from the mixing angle. Data from the Bayesian analysis of the related ratio data ^{7}Li/^{11}B are given at the 1 σ and 2 σ upper limits [10].

equation for the ν-density matrix that includes terms for the ν-SI as well as ν oscillations in both the vacuum and matter. The ν-SI turns out to surprisingly have a significantly larger effect on the ν-process in SN explosion than the MSW effect.

The heavy ν-isotopes are enhanced by a factor of 3–4, whereas the light isotopes are increased by only 5–30% in the IH case. The enhancement of the ν-isotopic abundances can be understood systematically by the contribution of ν_e in the high energy region above 17 MeV after the ν-SI near the ν sphere. The introduction of the ν-SI is shown to partially cancel the MSW effects on the ν spectral changes. Consequently, the ν-SI decreases the light-element abundances compared to the case without the ν-SI effect in the IH scheme. Therefore, the ν-SI should be taken into account along with the MSW effect when considering dense ν systems as the source for the ν-process and to constrain the neutrino MH. This work is based on an equi-partitioned neutrino flavor based on the Fermi-Dirac distribution. More general study considering the non-equivalent neutrino luminosity from the detailed neutrino transport calculations will appear elsewhere in near future.

References

[1] S. E. Woosley, D. H. Hartmann, R. D. Hoffman, and W. C. Haxton, Astrophys. J. **356**, 272 (1990).
[2] A. Heger, E. Kolbe, W. C. Haxton, K. Langanke, G. Martinez-Pinedo, and S. E. Woosley, Phys. Lett. B **606**, 258 (2005).
[3] T. Yoshida, T. Kajino, and D. H. Hartmann, Phys. Rev. Lett. **94**, 231101 (2005).
[4] Takashi Yoshida, Toshitaka Kajino, Hidekazu Yokomakura, Keiichi Kimura, Akira Takamura, and Dieter H. Hartmann, Phys. Rev. Lett. **96**, 091101 (2006).
[5] C. Kobayashi, N. Izutani, A. I. Karakas, T. Yoshida, D. Yong, and H. Umeda, Astrophys. J. **739**, L57 (2011).
[6] T. Hayakawa, K. Nakamura, T. Kajino, S. Chiba, N. Iwamoto, Myung-Ki Cheoun, and G. J. Mathews, ApJL **779**, 1 (2013).
[7] T. Hayakawa, Heamin Ko, Myung-Ki Cheoun, M. Kusakabe, T. Kajino, M. D. Usang, S. Chiba, K. Nakamura, A. Tolstov, K. Nomoto, M. A. Hashimoto, M. Ono, T. Kawano, and G. J. Mathews, Phy. Rev. Lett. **121**, 102701 (2018).
[8] T. Hayakawa, T. Kajino, S. Chiba, and G. J. Mathews, Phys. Rev. C **81**, 052801 (2010).
[9] S. M. Austin, A. Heger, and C. Tur, Phys. Rev. Lett. **106**, 152501 (2011).
[10] G. J. Mathews, T. Kajino, W. Aoki, W. Fujiya, and J. B. Pitts, Phys. Rev. D **85**, 105023 (2012).
[11] A. Sieverding, G. Martnez-Pinedo, L. Huther, K. Langanke, and A. Heger, Astrophys. J. **865**, no. 2, 143 (2018).

[12] T. Iizuka, Y. J. Laib, W. Akram, Y. Amelin, and M. Schoenbaechler, Earth Plan. Sci. Lett. **439**, 172 (2016).
[13] H. Becker and R. J. Walker, Chem. Geol. **196**, 43 (2003).
[14] Julien Serreau and Cristina Volpe, Phys. Rev. D **90**, 125040 (2014).
[15] G. Sigl and G. Raffelt, Nucl. Phys. **B** 406, 423 (1993).
[16] Y. Pehlivan, A. B. Balantekin, Toshitaka Kajino, and Takashi Yoshida, Phys. Rev. D **84**, 065008 (2011).
[17] G. L. Fogli, E. Lisi, A. Mirizzi, and D. Montanino, Phys. Rev. D **68**, 033005 (2003).
[18] T. Yoshida, T. Suzuki, S. Chiba, T. Kajino, H. Yokomakura, K. Kimura, A. Takamura, and D. H. Hartmann, Astrophys. J. **686**, 448 (2008).
[19] H. Sasaki, T. Kajino, T. Takiwaki, T. Hayakawa, A. B. Balantekin, and Y. Pehlivan, Phys. Rev. **D** 96, 043013 (2017).
[20] S. Chakraborty, T. Fischer, A. Mirizzi, N. Saviano, and R. Tomas, Phys. Rev. Lett. **107**, 151101 (2011).
[21] Sayad Abbar and Huaiyu Duan, Phys. Lett. **B** 751, 43 (2015).
[22] M. R. Wu, Y. Z. Qian, G. Martinez-Pinedo, T. Fischer, and L. Huther, Phys. Rev. D **91**, 065016 (2015)
[23] T. Shigeyama, K. Nomoto, and M. Hashimoto, Astrophys. Astronm. **196**, 141 (1988).
[24] Y. Kikuchi, M. Hashimoto, M. Ono, and F. Fukuda, Prog. Theor. Exp. Phys. **2015**, 063E01 (2015).
[25] S. Blinnikov, P. Lundqvist, O. Bartunov, K. Nomoto, and K. Iwamoto, Astrophys. J. **532**, 1132 (2000).
[26] Myung-Ki Cheoun, E. Ha, T. Hayakawa, S. Chiba, K. Nakamura, T. Kajino, and G. J. Mathews, Phys. Rev. C **85**, 065807 (2012).
[27] Myung-Ki Cheoun, Eunja Ha, T. Hayakawa, Toshitaka Kajino, and Satoshi Chiba, Phys. Rev. **C** 82, 035504 (2010).
[28] O. Iwamoto, N. Iwamoto, S. Kunieda, F. Minato, and K. Shibata, Nucl. Data Sheets **131**, 259 (2016).
[29] K. A. Olive *et al.* [Particle Data Group], Chin. Phys. C **38**, 090001 (2014).
[30] T. Kawano, P. Talou, M. B. Chadwick, and T. Watanabe, J. Nucl. Sci. Technol. **47**, 462 (2010).
[31] Motohiko Kusakabe, Myung-Ki Cheoun, K. S. Kim, Masa-aki Hashimoto, Masaomi Ono, Ken'ichi Nomoto, Toshio Suzuki, Toshitaka Kajino, and Grant J. Mathews, Astrophys. J. **872**, 164 (2019).